Journal of Physics: Conference Series **572** (2014) 012048 doi:10.1088/1742-6596/572/1/012048

Effects of nickel ions implantation and subsequent thermal annealing on structural and magnetic properties of titanium dioxide

I R Vakhitov[1*], N M Lyadov[2], V F Valeev[2], V I Nuzhdin[2], L R Tagirov[1], R I Khaibullin[1,2]

[1] Institute of Physics, Kazan Federal University, Kazan, Russian Federation
[2] Laboratory of Radiation Physics, Zavoisky Physical-Technical Institute of Russian Academy of Science, Kazan, Russian Federation

*E-mail: ujay@mail.ru

Abstract. Wide bandgap semiconducting rutile (TiO_2) doped with 3d-elements is a promising material for spintronic applications. In our work a composite material of TiO_2:Ni has been formed by using implantation of Ni^+ ions into single-crystalline (100)- and (001)- plates of TiO_2. Sub-micron magnetic layers of TiO_2 containing nickel dopant have been obtained at high implantation fluence of 1×10^{17} ion/cm^2. A part of the implanted samples was then annealed in vacuum at different temperatures T_{ann} = 450-1200 K for 30 min. The influence of the implantation fluence, crystalline orientation, as well as subsequent annealing on the structural and magnetic properties of the nickel-implanted TiO_2 have been investigated by using X-ray photoelectron spectroscopy, scanning electron microscopy and coil magnetometry techniques.

1. Introduction

Synthesis and study of a new class of materials known in literature as oxide diluted magnetic semiconductors (DMS) have great scientific interest today. It is new class of semiconductors, considered as most promising material for applications in rapidly developing branches of science like spintronics and magnetic optoelectronics [1,2]. Various techniques have been developed for synthesis of DMS systems. Among them ion implantation is a promising method [3]. This refers both to technological capabilities of the method, as well as wide implementation of this technology in manufacturing of modern integrated circuits. Earlier, we studied semiconducting rutile TiO_2 single crystals implanted by cobalt ions in a wide range of implantation fluencies [4-6]. It was shown that depending on the implantation regimes, crystallographic orientation of the substrate, substrate temperature during the irradiation, either anisotropic ferromagnetic nanocomposite material TiO_2:Co, or isotropic DMS $Co_xTi_{1-x}O_{2-\delta}$ with a high Curie temperature (~700 K) were obtained [6-8]. In this paper we present results of the study of Ni implantation and subsequent thermal annealing on the structural and magnetic properties of rutile TiO_2.

2. Experimental details

Ni^+ ions with the energy of 40 keV were implanted into (100)- and (001)- oriented plates of single crystalline rutile TiO_2 to the fluence of 1×10^{17} ion/cm^2 at ion current density of 8 μA. The implantation was carried at room temperature of TiO_2 substrate by using ILU-3 ion accelerator (ZPhTI

of RAS). Then, the implanted samples were annealed under high vacuum ~10^{-6} Torr at different temperatures ($T_{ann.}$) in the range from 450 to1200 K for the fixed time interval of t_{ann} = 30 min.

The elemental composition and surface morphology were studied by using scanning electron microscope (SEM) Carl Zeiss EVO'50 equipped with X-ray energy-dispersive spectrometer Oxford INCA Energy 330. The valences of Ni and Ti ions were determined by X-ray photoelectron spectroscopy (XPS). XPS measurements were performed in a UHV chamber (base pressure ~ 3×10^{-10} mbar) equipped with a monochromatic Mg K_α X-ray source operated at 12.5 kV and 250 W, and a Phoibos 150 hemispherical energy analyzer (all from SPECS). The energy analyzer was operating with the pass energy of 25 eV and the step size of 0.1 eV. All spectra were analyzed by using the CasaXPS software [9]. Peak shifts due to any apparent charging were calibrated with the carbon 1s peak set to 284.6 eV. After the calibration, the background from each spectrum was subtracted using a Shirley-type background. Magnetic properties of the samples were studied using the experimental home-made coercive magnetometer. The dependences of the induced and remanent magnetic moments on magnetic field were recorded at room temperature upon sweep of magnetic field up to 500 mT. The magnetic field was applied either in the plane of the sample (in-plane geometry) or perpendicular to the plane of the sample (out-of-plane geometry). Diamagnetic contribution from the substrate was subtracted during the processing of the results. The registered magnetic moment was normalized by the number of nickel atoms contained in the samples.

3. Results and discussions

SEM and XPS elemental analysis of the implanted rutile has shown the presence of only the implanted nickel and structure forming elements: titanium and oxygen with a reduced content of the last. This indicates that main radiation defects in titanium dioxide are oxygen vacancies. Areal concentration of the implanted impurity does not change after the thermal annealing. As a result of the SEM study it was found that the surface of the samples is generally smooth without any new growths both after ion implantation and thermal annealing.

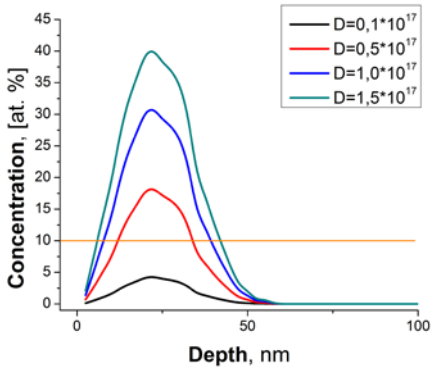

Figure 1. Depth profiles of nickel concentration at different values of the implantation fluence.

Computer package SRIM-2008 [10] was used to calculate depth distribution of nickel implanted into the rutile structure TiO_2 matrix that has density equal to 4.24 g/cm^3. Figure 1 shows that the concentration of Ni implants increases with increasing the implantation fluence. At the fluence more than 0.2×10^{17} ion/cm^2 the concentration of the implanted impurity exceeds the average value of maximum solubility of cobalt in the rutile matrix, which is equal to ~10 at.% (orange line in fig. 1). This means that at higher values of implantation fluence the implanted impurity may be found in the form of nanosize particles of nickel metal as the solubility limit is exceeded.

XPS measurements were taken in order to check valence states of titanium and nickel in the Ni-implanted TiO_2 samples. First of all, the analysis of XPS spectra have shown that there is no influence

of orientation of the samples on the XPS spectra of Ti 2p and Ni 2p. Figure 2 shows high-resolution XPS spectrum of the Ti 2p region for (100) Ni implanted TiO_2 sample and the same sample subsequently annealed in vacuum at 1050 K, respectively. The Ti $2p_{3/2}$ and Ti $2p_{1/2}$ peaks are identified at 458.1 eV and 463.8 eV, respectively. The splitting of the binding energy between Ti $2p_{3/2}$ and Ti $2p_{1/2}$ core levels is about 5.7 eV, which matches the reported value of 5.7 eV [11]. This indicates a valence state of Ti^{4+} in TiO_2 [11].

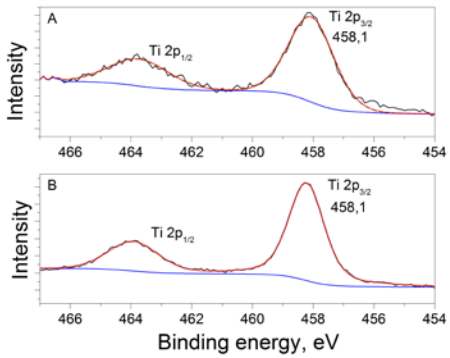

Figure 2. High-resolution XPS spectrum of the Ti 2p region for (A) (100)-oriented rutile implanted by Ni^+ ions and (B) subsequently annealed in vacuum at 1050 K.

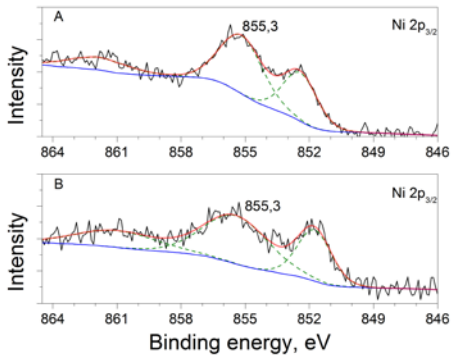

Figure 3. High-resolution XPS spectrum of the Ni $2p_{3/2}$ region for (A) (100)-oriented rutile implanted by Ni^+ ions and (B) subsequently annealed in vacuum at 1050 K.

Figure 3 shows Ni 2p core level X-ray photoelectron spectra of (100)-oriented TiO_2 samples: as-implanted and post-annealead (T_{ann}=1050 K) sample, respectively. From our analysis of the chemical states of nickel, the Ni $2p_{3/2}$ main peak located at 855.3 eV (corresponding to the Ni^{2+} in $NiCO_3$) and more weak peak was assigned to Ni^0 ("pure" Ni metal binding energy – 852.4 eV) [11]. This indicates that the chemical valence of Ni in as-implanted sample is 0 (metal) or 2+ (ion). The results for the post-annealed Ni-implanted TiO_2 are in agreement with the literature data for the Ni $2p_{3/2}$ main peak located at 855.3 eV that corresponds to Ni^{2+} ions.

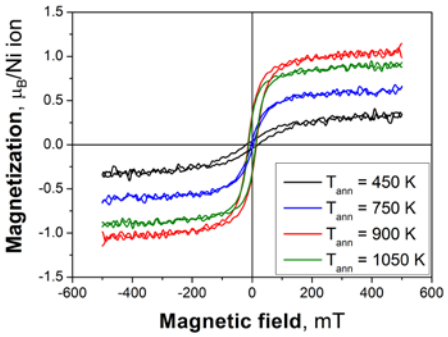

Figure 4. The magnetic hysteresis curve evolution for Ni-implanted TiO_2 after the annealing of the sample in high vacuum at different temperatures ($T_{ann.}$).

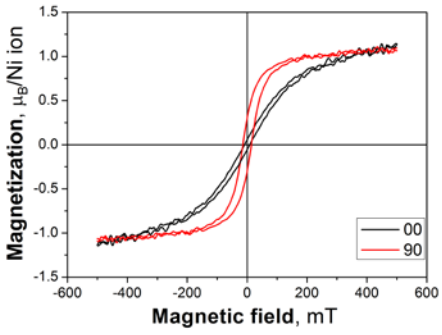

Figure 5. The out-of-plane hysteresis curves of the (001)- TiO_2 sample implanted with nickel ions and then annealed in vacuum at 900 K. The curves for two polar angles of θ=0º and θ=90º are shown.

Magnetic measurements have shown that the virgin (non-implanted) TiO_2 plates reveal diamagnetic response. The measurements of the as-prepared samples implanted with nickel ions have shown superparamagnetic behavior for all samples in any orientation. However, subsequent thermal annealing in vacuum resulted in the appearance of room temperature ferromagnetism of the samples. Figure 4 shows magnetic evolution of Ni-implanted (100) TiO_2 samples after the annealing in vacuum at different temperatures ($T_{ann.}$). The magnetization increases with increasing the temperature of annealing. It reaches maximum of about 1.1 μ_B at the annealing temperature of $T_{ann.}$ = 900 K. After that, the saturation magnetization starts to the decrease with following increase of the annealing temperature.

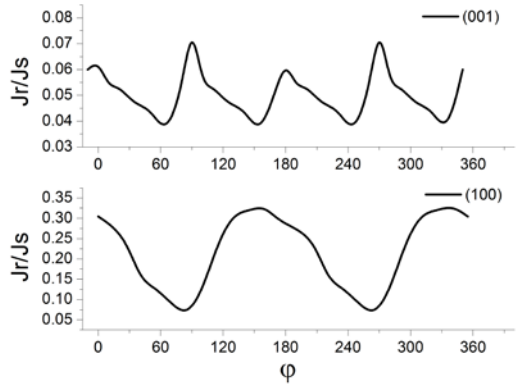

Figure 6. The in-plane azimuthal angular dependences of the ratio of remanent magnetic moment (J_r) to the spontaneous saturation moment (J_s) for different orientations of the post-annealed Ni-implanted TiO_2 plates.

Figure 5 shows out-of-plane magnetization curves of the (001)-oriented TiO_2 plate implanted with nickel ions and subsequently annealed in vacuum at 900 K (the curve for (100) orientation is the same). These dependences show that the samples demonstrate shape anisotropy that is typical for ferromagnetic thin films. Namely, samples quickly and easily magnetize to saturation by an applied magnetic field in the plane (θ =90º) of the plate. In contrast, application of magnetic field along the normal to the plate (θ =0º) does not saturate the sample even at maximum magnetic field of 500 mT.

In addition, the samples show magneto-crystalline anisotropy in the plane of the Ni-implanted plate of TiO_2 after high-temperature annealing at $T_{ann.}$ =750 K. Figure 6 displays in-plane angular dependences of the ratio of the remanent magnetic moment (J_r) to the spontaneous saturation moment (J_s) in the TiO_2 plates with different orientations, (100) and (001), respectively. It is clearly seen that the (100)-oriented samples reveal two-fold symmetry of the ferromagnetic response, and the (001)-oriented plates of TiO_2 show four-fold magnetic anisotropy. Taking into account the tetragonal symmetry of rutile, in which [100] and [001] are the axes of second and fourth orders of symmetry, respectively, we can conclude that the ion-synthesized DMS material TiO_2:Ni is coherently embedded in rutile matrix. Both the shape and magneto-crystallographic anisotropies become less pronounced with increasing the annealing temperature, and disappear completely at 900 $T_{ann.}$=1200 K for (100)-oriented TiO_2 plates and at $T_{ann.}$ = 900 K for (001) orientation of the samples.

It is important to note that the similar magnetic crystallographic anisotropies were early observed in single crystalline rutile (TiO_2) heavily implanted with Co [5, 12, 13], Fe [14, 15] or Ni [16]. Authors of these works have shown that in-plane magnetic anisotropy in 3d-ion implanted TiO_2 originates from secondary phases: metal nanoclusters of cobalt, iron or nickel grown coherently in the rutile matrix. Therefore, we may conclude that the magnetic crystallographic anisotropy observed in our post-

annealed Ni-implanted samples could be related to the formation of magnetic Ni nanoparticles with orientations correlated with theTiO_2 rutile structure.

4. Conclusion

The effects of Ni ions implantation and subsequent vacuum annealing on structural and magnetic properties of TiO_2 single-crystalline plates were studied. XPS measurements show the mixed, 2+ and 0, valence states of Ni which corresponds to Ni^{2+} ions and Ni metal nanoparticles implanted in rutile matrix. All as-implanted plates of TiO_2 reveal superparamagnetic response at room temperature. Subsequent thermal annealing of the samples in vacuum leads to room temperature ferromagnetism with magnetic shape anisotropy characteristic for thin magnetic films. Strong influence of the crystallographic orientation of the TiO_2 plates on the in-plane magnetic anisotropy of post-annealed samples, was observed: (100) TiO_2 plate showing two-fold, and (001) TiO_2 – four-fold symmetry of the ferromagnetic response, respectively.

Acknowledgments

This work was funded by the subsidy allocated to Kazan Federal University for the state assignment in the sphere of scientific activities, and support in part by Russian Youth-Innovation Program U.M.N.I.K. is acknowledged.

References

[1] Janisch R, Gopal P, Spaldin N 2005 *J. Phys.: Cond. Matter.* **17** R657
[2] Prellier W, Fouchet A, Mercey B 2003 *J. Phys.: Cond. Matter.* **15** R1583
[3] Theodoropoulou N, Hebard A, Chu S, Overberg M, Abernathy, Pearton S, Wilson R, Zavada J 2002 *J. Appl. Phys.* **91** 7499
[4] Khaibullin R, Tagirov L, Rameev B, Ibragimov Sh, Yildiz F, Aktas B 2004 *J. Phys.: Cond. Matter.* **16** L443
[5] Khaibullin R, Ibragimov Sh, Tagirov L, Popok V, Khaibullin I 2007 *Nucl. Instr. and Meth. in Phys. Res. Sect. B* **257** 369
[6] Akdogan N, Nefedov A, Zabel H, Westerholt K, Becker H, Somsen C, Gok S, Bashir A, Khaibullin R, Tagirov L 2009 J. Phys. D: Appl. Phys. **42** 115005
[7] Khaibullin R, Tagirov L, Ibragimov Sh, Valeev V, Nuzhdin V, Osin Yu, Achkeev A, Faizrakhmanov I, Cherkashin N 2007 *Kazan. Gos. Univ. Uchen. Zap. Ser. Fiz.-Mat. Nauki* **149** 31 (English abstract is accessible at http://mi.mathnet.ru/eng/uzku/v149/i3/p31)
[8] Achkeev A, Khaibullin R, Tagirov L, Mackova A, Hnatowicz V, Cherkashin N 2011 *Phys. Solid State* **53** 543
[9] CasaXPS: Processing Software for XPS, AES, SIMS and More (http://www.casaxps.com)
[10] Ziegler J, Biersack J, Littmark U 1985 (http://www.srim.org/#SRIM)
[11] Wagner C, Riggs W, Davis L, Moulder J, Muilenberg 1979 *Handbook of X-ray Photoelectron Spectroscopy* (Minnesota, Perkin-Elmer Corporation)
[12] Akdogan N, Rameev B, Khaibullin R, Westphalen A, Tagirov L, Aktas B, Zabel H 2006 J. *Magn. Magn. Mater.* **300** e4
[13] Pinto J, Cruz M, da Silva R, Alves E, Gonzalez R, Godinho M 2007 Eur. Phys. J. B **55**, 253
[14] Vakhitov I, Nujdin V, Osin Yu, Khaibullin R 2010 *Kazan. Gos. Univ. Uchen. Zap. Ser. Fiz.-Mat. Nauki* **152** 7 (English abstract is accessible at http://mi.mathnet.ru/eng/uzku/v152/i3/p7)
[15] Zhou S, Talut G, Potzger K, Shalimov A, Grenzer J, Skorupa W, Helm M, Fassbender J, Cizmar E, Zvyagin S, Wosnitza J 2008 *J. Appl. Phys.* **103** 083907
[16] Cruz M, da Silva R, Pinto J, Borges R, Franco N, Casaca A, Alves E, Godinho M 2013 *J. Magn. Magn. Mater.* **340** 102